ARTICLE NO. 79-0592R

J80-078

20001
20007

Discrete Noise Spectrum Generated by an Acoustically Excited Jet

Valdis Kibens*
McDonnell Douglas Corporation, St. Louis, Mo.

The shear layer of an axisymmetric air jet ($Re = 50{,}000$) was perturbed using a symmetrical acoustic excitation chamber surrounding the nozzle at a frequency $f_e = f_s$, where f_s is the shear-layer instability frequency. The excitation organized the large-scale structures in the shear layer into a sequence of three successive vortex-pairing stages at fixed streamwise locations, producing the subharmonic frequencies $f_e/2, f_e/4$, and $f_e/8$. The pressure spectra in the near field and the acoustic spectra in the far field contained peaks at the frequencies corresponding to the rate of formation of large-scale turbulent structures through vortex pairing. The broadband noise of the excited jet was reduced by as much as 10 dB compared with the non-excited jet.

Introduction

MAJOR problems in jet-engine exhaust-noise suppression are encountered at the lower end of the noise spectrum where the acoustic wavelengths approach the engine exhaust passage dimensions. This range of frequencies is generated by turbulent eddies whose size is of the order of the jet-stream radius. Jet noise reduction in this frequency range is expected to involve devices and methods that modify the acoustic field by shaping the distribution of turbulent scales in the flowfield. Thus, there is increasing motivation to establish the relationship between the detailed turbulent flow characteristics of the proposed devices and the features of the acoustically propagating pressure waves generated by the flow.

The need to suppress jet-noise frequencies in the range $0.2 \leq St \leq 0.5$, where St is the nondimensional frequency fD/U_0, D the jet diameter, and U_0 the jet exit velocity, has concentrated attention on the properties of the large-scale organized motion in the first six diameters of a jet flowfield downstream of the exit plane. Crow and Champagne[1] demonstrated that the formation of large-scale coherent flow structures can be enhanced by perturbing the flow at frequencies characteristic of their passage rate. They showed that by imposing a sinusoidal planar disturbance on the jet exit flow at a nondimensional frequency $St = 0.3$, the flow could be organized so that its dominant dynamic feature was a succession of highly organized coherent flow regions in the form of axisymmetric vortices. Crow and Champagne[1] suggested that the organized structure of the jet flowfield may play a major role in the generation of the acoustic field of the jet. Extensive measurements in two-dimensional shear layers were made by Browand and Winant[2] as well as Brown and Roshko[3] to establish the mechanisms of vortex formation and development. They observed that shear-layer growth occurs through a sequence of vortex pairing events in which larger scales are formed in discrete steps through the merging of one or more smaller vortex structures. Browand and Weidman[4] used conditional sampling techniques to show that the vortex pairing mechanism also persists at higher Reynolds numbers, but is randomized in phase so that conventional data analysis cannot identify the process properly. The process of vortex pairing in axisymmetric jets, as well as the effect of artificial forcing at various frequencies, has been studied qualitatively and quantitatively in flow visualization studies by Browand et al.[5] Michalke and Fuchs[6] considered the various modes of large-scale motion that can be sustained by a jet flow by separating the unsteady pressure field into axisymmetric and higher order azimuthal components. Fuchs and Michel[7] summarized the experimental evidence linking jet noise to coherent large-scale turbulent noise sources and reported that both in a model scale jet and a jet engine at Mach numbers as high as $M = 0.69$, the measurements of azimuthal coherence of the jet near-field pressure indicate that well over one-half of the fluctuating energy is contained in the axisymmetric mode.

The role of large-scale structures in generating the acoustic pressure field has been observed to be significant at high subsonic Mach numbers by Sarohia.[8] McLaughlin et al.[9] reported that coherent flow instabilities produce a dominant portion of the noise in low-Reynolds-number jets (5000–100,000) at Mach numbers of 1.5 and 2.3. The measurements by Lau et al.,[10] Maestrello,[11] and Petersen et al.[12] represent attempts to relate jet noise to specific noise-generation events and discretely identified turbulent eddies.

The use of excitation of the jet flowfield has become widely used for investigating the characteristics of both the flowfield and the acoustic field. The flowfield of a low-subsonic axisymmetric jet under excitation has been investigated by Hussain and Zaman.[13] Extensive experimental and theoretical work on the spatial growth of wavelike disturbances in jet shear layers has been performed by Chan.[14] His experimental technique involved wide use of acoustic forcing, and he has also investigated the growth of helical waves in the jet shear layer. McLaughlin et al.[9] used the excitation method for supersonic jet studies. The effect of excitation on the acoustic field of subsonic jets was the main object of the investigations by Bechert and Pfizenmaier[15] and by Moore.[16] Bechert and Pfizenmaier excited the jet by placing four acoustic drivers at radial positions outside the jet nozzle, communicating to the flow through gauze-covered openings in the nozzle wall. The variation of phase among the four drivers permitted them to vary the excitation mode number. They found that excitation of the jet in the axisymmetric mode at $St \cong 0.5$ amplified the broadband jet noise at $M = 0.6$ by 6 to 7 dB. The increase in far-field broadband noise upon excitation of the jet also was reported by Moore.[16] He

Presented as Paper 79-0592 at the AIAA 5th Aeroacoustics Conference, Seattle, Wash., March 12-14, 1979; submitted April 6, 1979; revision received Sept. 14, 1979.

Index categories: Aeroacoustics; Jets, Wakes, and Viscid-Inviscid Flow Interactions.

*Scientist, McDonnell Douglas Research Laboratories. Member AIAA.

concluded that manipulation of the coherent structure distribution in the jet could produce significant changes in the jet noise field, although it did not generate noise directly.

Experimental Method and Apparatus

The object of this study was to generate a jet flowfield in which the role of large-scale structures in the flowfield and the acoustic field could be studied unambiguously. Crow and Champagne[1] reported that the application of excitation methods became increasingly difficult for laboratory-scale experiments in air above $Re=50{,}000$. For this reason we selected 50,000 as the Reynolds number for the present experiment. The method of excitation differed from those discussed in the introduction.[9,13,15,16] Instead of employing an excitation source located in the supply stream which produces a planar oscillation of the jet stream at the nozzle exit, a confined excitation source external to the flow was used as shown schematically in Fig. 1. An azimuthally coherent perturbation was introduced locally at the nozzle exit through a thin slit surrounding the nozzle. The excitation wave was formed in a peripheral exciter chamber driven from a loudspeaker enclosure, connected to the exciter chamber through flexible tubing. The exciter chamber was divided into four segments, each driven from an individual supply hose from the same driver source. This method produced an azimuthally coherent pressure wave at the exciter chamber exit. The nozzle exit diameter was 2.54 cm. The width of the acoustic-driver exit slit was 0.25 cm, and the direction of the impinging wave was 15 deg from the normal to the jet axis.

The intent of this excitation method was to employ the gain characteristics of the shear layer to control its development by injecting a perturbation signal at the most highly amplified frequency and to use the distribution of the large-scale coherent structures in the developing shear layer to supply the perturbation spectrum for the entire jet flowfield. In this method, the frequencies selected are not restricted to cavity resonance frequencies as occurs for methods in which the acoustic driver is located in the settling chamber of the flow. Also, the nearly radial impingement of the excitation wave on the shear layer introduces a small radial velocity perturbation in the shear layer at the point of highest sensitivity, namely, the point of shear-layer separation from the nozzle exit corner. The excitation level was adjusted to produce a sound pressure level of 90 dB at the exciter exit as measured by an 0.3-cm-diam B&K microphone in the absence of flow. This excitation level was sufficiently low so that a signal at the excitation frequency could not be observed by a hot wire placed in the excited flow either on the exit plane centerline or in the shear layer at the exit of the excitation chamber.

A high-pressure air source was used to provide the flow. The settling chamber consisted of a high-angle diffuser containing a series of screens, a honeycomb with a passage length of 0.127 m and cell diameter of 0.0003 m followed by two screens of decreasing mesh size, and a machined contraction nozzle block with an overall contraction ratio of 144:1. The nozzle walls at the exit plane were parallel to the centerline.

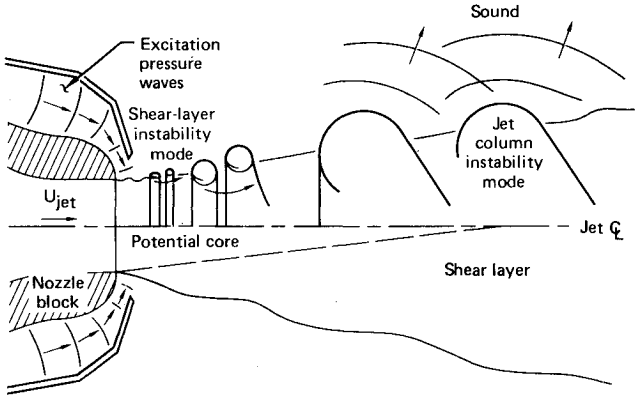

Fig. 1 Acoustic excitation of jet shear-layer structure.

The acoustic far-field measurements were performed in an anechoic chamber located at the NASA Ames Research Center. The chamber dimensions inside the wedge tips were $6\times8\times3$ m high. The wall construction provided sound-pressure attenuation of 25 dB at 63 Hz to 62 dB at 2000 Hz. The inside of the chamber was lined with polyurethane-foam wedges which were 0.6-m deep from base to tip and provided more than 99% acoustical absorption at 150 Hz. Acoustical measurements were taken with a linear array of six 12.7-mm-diam B&K microphones placed on a line parallel to the jet axis. The microphone locations were at streamwise distances $x/D=0$, 10, 20, 30, 40 and 50 from the jet exit plane, and the distance of the array from the jet axis was $R/D=30$, 40 and 50. The acoustical data were recorded on magnetic tape for subsequent analysis.

Description of Flowfield

The flowfield was investigated using hotwire measurements.[19] A high-speed photography flow visualization technique was used, consisting of an optical system with two 120.3-cm mirrors used in a shadowgraph mode in conjunction with a high-intensity light source and a high-speed movie camera operated at 5000 frames/s. The contrast was obtained by adding helium into the airflow at a point upstream of the system settling chamber at a concentration of approximately 3% of the total mass flow rate.

The jet velocity was constant across the exit plane. The boundary layer at the nozzle exit was laminar, with a thickness of $\delta=0.08$ cm. The exit turbulence level at the centerline was $\sqrt{\tilde{u}'^2}/U_0=0.0012$. The measurements of principal interest concerned the distribution of large turbulent scales in the shear layer and in the jet column throughout the region in which coherent structures could be observed, i.e., $0\le x/D\le6$. The nonexcited-jet shear layer was investigated using hot-wire measurements. A rapid increase of periodic fluctuations was observed in the shear layer at $r/D=0.5$ from $0\le x/D\le1.0$; the fluctuation level for $x/D>1$ decayed into increasingly random turbulent motion. The instability frequency, f_s, of the wave observed in the shear layer corresponded closely to that predicted by the linear theory of Michalke.[17]

Excitation was then applied at a frequency $f_e\cong f_s$. The hot-wire signals were analyzed for frequency content by forming the autocorrelation function $R_{uu}=u(t)u(t-\tau)$, and systematically taking the delay time to the first peak of R_{uu} to be the period of the passage rate of the eddies at the hot-wire location. The results are summarized in Fig. 2. The frequencies observed in the shear layer are presented in the form $St=fD/U_0$ vs stream-wise distance x/D. Excitation enhanced and stabilized the large axisymmetric eddies in the shear layer. The perturbations were amplified in the shear layer and formed axisymmetric vortex rings which paired three times, each pairing event occurring at a fixed streamwise location. The vortex pairing sequence produced frequencies $f_e/2$, $f_e/4$, and $f_e/8$ in the flowfield. Figure 2 shows the distribution of dominant frequencies over the first eight diameters of the jet shear layer. The vortex pairing events occurred in the region between the dashed vertical lines in Fig. 2, and in these regions frequencies corresponding to both the single and merged vortices were visible. The scale of the shear-layer structures doubled at each step. The shear-layer dynamics increasingly influenced the core flow fluctuations with axial distance until at $x/D=3$ the fluctuating flow in the entire jet column was dominated by the large-scale motion at the frequency $f_e/8$ associated with the fourth stage in the vortex pairing cascade. The velocity fluctuations on the centerline are indicated by the square symbols and show that

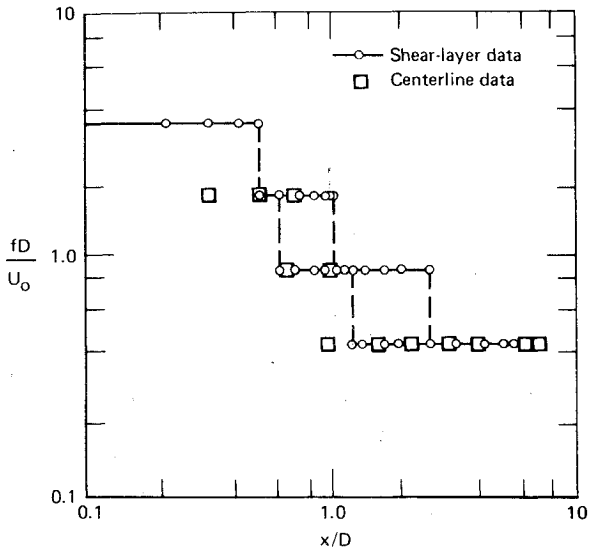

Fig. 2 Nondimensional frequency vs x/D for acoustically excited jet. $Re = 5 \times 10^4$. St_e = nondimensional excitation frequency = 3.54.

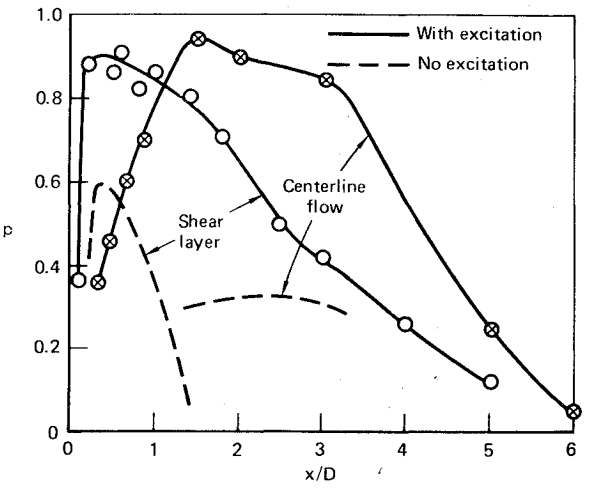

Fig. 3 Fraction p of turbulent energy contained by coherent motion (based on longitudinal velocity fluctuation component).

fluctuations on the centerline were induced by the large scales at locations well upstream of the axial position at which those scales were formed in the shear layer.

Figure 3 shows the fraction of turbulent energy contained by the coherent motion, calculated by graphically decomposing the autocorrelation function of a particular signal into contributions from the random and periodic parts. For the nonexcited jet the significant coherent motion in the shear layer was confined to $0 \leq x/D \leq 1$ and reached a maximum of 60% of the total energy at the location of the first pairing of the vortices. The level of coherence dropped rapidly thereafter. With excitation, however, as much as 90% of the turbulent energy was associated with the large-scale structures in the shear layer at the location of the first pairing, and the energy level was 50% at $x/D = 2.5$ where the last pairing had been completed. The shear layer influenced the flow on the centerline so that the dynamic properties of the excited jet could be regarded as a quasi-deterministic motion organized by the basic excitation frequency f_e and the series of subharmonics derived from f_e by the vortex pairing cascade in the shear layer.

Figure 4 shows two frames from the flow visualization movies demonstrating the effect of excitation on the flow. The frames selected are for flow through a 6.35-cm nozzle at 12.2 m/s. The development of the vortices is discernible for the nonexcited case in Fig. 4a; the coherent part of the motion is clearly axisymmetric, and several stages of development are visible. In Fig. 4b the exciter is operated at $f_s/2$. At this frequency the maximum effectiveness of the exciter in organizing the flow is obtained. The density effect caused by the addition of approximately 3% helium by mass required to provide shadowgraph contrast lowered the excitation efficiency so that the coherence in the visualized flow is less than in the flow with air alone. The flow visualization movies confirm that excitation fixes the pairing location positions and that the regions indicated in Fig. 2 by the dashed lines correspond to the locations of vortex pairing.

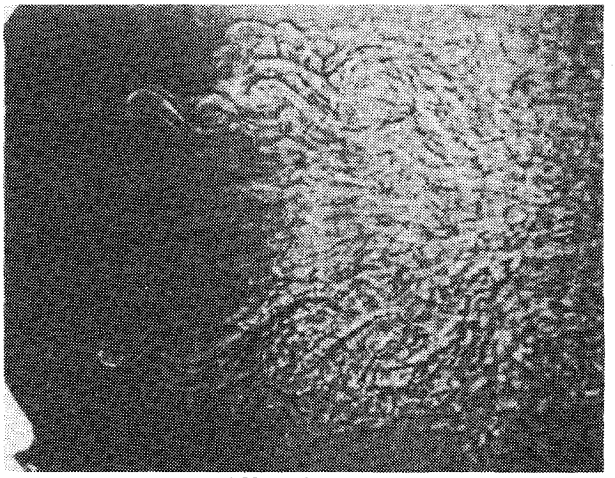

a) No excitation

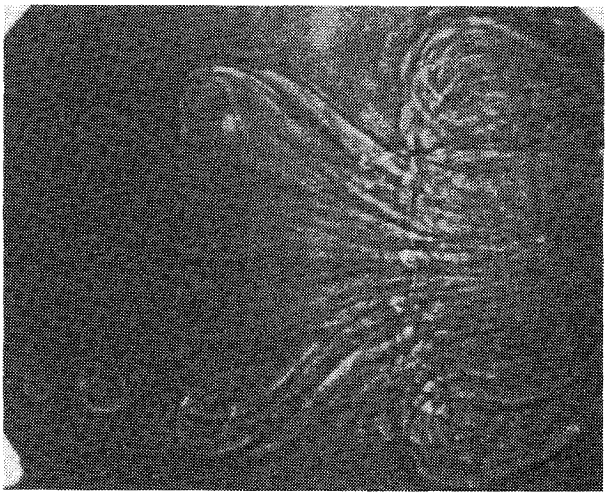

b) With excitation

Fig. 4 Shadowgraph images showing coherent turbulent structure in nozzle jet flow; $Re = 50{,}000$.

Acoustic Field Characteristics

Figure 5 shows the effect of excitation on the near-field pressures. For the nonexcited case, the pressure field at the reference microphone position $(x/D, R/D) = (1,1)$ exhibited a broad peak centered on $St = 0.37$. Excitation of the shear layer at the frequency $f_e D/U = 3.7$ reflected in the pressure field the increased organization seen in the flowfield in Fig. 2. The frequencies observed in the flowfield that are associated with formation and the passage of the vortex ring cascade appeared in the spectrum of the near-field microphone as discrete spectrum peaks at the frequencies $f_e/2^n, n = 0,1,2,3$. The intensity of the peak of f_e remained unchanged when the flow was turned off, indicating that the flowfield did not radiate at the frequency f_e. The intermediate spectrum peaks at $St = 1.4$, 2.3, and 2.8 are integer multiples of $f_e/8$, in-

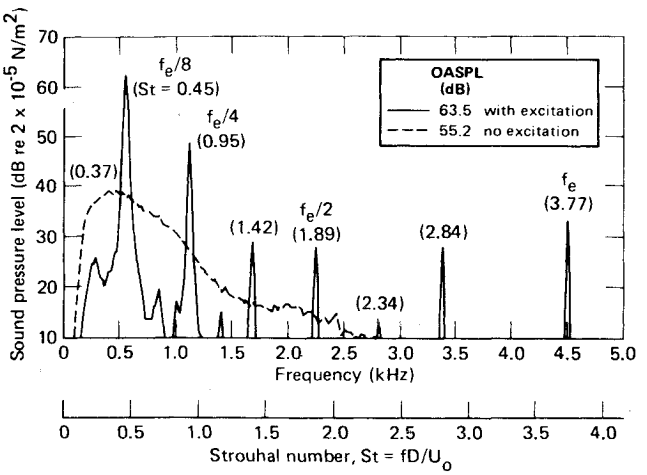

Fig. 5 Near-field pressure spectrum at position $(x/D, R/D)=(1,1)$; $U_0=30.5$ m/s; $f_e=4525$ Hz.

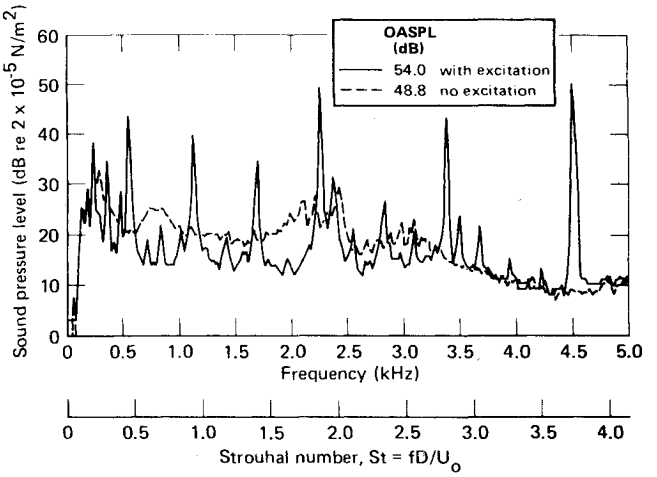

Fig. 6 Acoustic pressure spectrum at (0,30); $U_0=30.5$ m/s; $f_e=4525$ Hz.

dicating the presence of nonlinear interactions between the frequencies corresponding to the observed vortex-passage frequencies in the flowfield.

Figure 2 shows that at the streamwise location of the reference microphone, $x/D=1$, the second vortex pairing is almost complete, but the third has not begun. Nevertheless, the pressure field at (1,1) was dominated by the spectrum peak at $f_e/8$, thus suggesting that the entire vortex pairing process occurs against a dominant fluctuating pressure background at a frequency corresponding to the rate of formation or dissolution of the largest scales formed by this process. Laufer and Monkewitz[18] have suggested that the pressure fluctuations caused by the largest scales in a jet at the end of the potential core synchronize the formation and growth of the shear-layer vortices near the exit plane. The overall pressure level at the reference microphone location increases by 8.3 dB upon excitation.

The excitation frequency for all results reported herein was initially set equal to the measured shear-layer instability frequency, f_s, and adjusted slightly to give maximum energy in the coherent flowfield. The shear layer constituted a narrow band-pass amplifier in that a departure from optimum excitation frequency of approximately 10% was sufficient for the flow to revert to essentially nonexcited conditions. The flowfield data and the acoustic data were obtained in different facilities. The difference in excitation frequencies between Fig. 2 and, say, Fig. 5, reflects a slight difference in the values of mass flow rates between the two tests. The radial velocity fluctuation level at the shear-layer origin was not measured. The low level of excitation used, resulting in no measurable u' component either at the exciter exit or in the exit plane of the nozzle, suggests that the excited jet exhibits properties which to a lesser degree are also present in a nonexcited jet. The excited jet should not be regarded as being in a process of transition from laminar flow. The nonexcited jet may be regarded as containing an underlying degree of organization which is overlooked using conventional mean measurements and which is intensified by the phase locking of the excitation process.

The correspondence in frequency between the flowfield measurements and the near-field pressure spectrum was exact for the excited case. Note, however, that the spectrum peak at $f_e/8$ for the excited case did not coincide with the location of the maximum in the broad peak for the nonexcited case. The following heuristic argument could explain this mismatch. Two basic mechanisms govern the selection of dominant frequencies in the jet flowfield. The first is the formation of waves and their rollup into vortices at the shear-layer instability frequency f_s which initiates the subsequent pairing steps by the vortices. The frequency f_s, which is basic to this

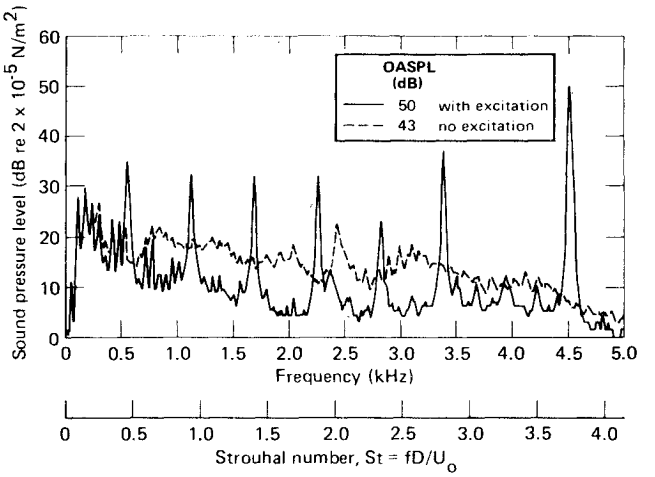

Fig. 7 Acoustic pressure spectrum at (50, 50); $U_0=30.5$ m/s; $f_e=4525$ Hz.

mechanism, is a function of the shear-layer momentum thickness, the jet velocity and the jet radius. The second mechanism is the jet-column instability; it determines the frequency f_j at which the largest scales in the jet are formed in the absence of a driving mechanism, as a function of the jet diameter and the jet velocity. This frequency has been observed for a wide range of Reynolds numbers and Mach numbers from $0.2 \leq f_j D/U \leq 0.5$. For the nonexcited case, the energy of the coherent motion in the shear layer decreases rapidly after the first pairing, and the two mechanisms can be considered independent, or only weakly coupled. When the shear layer is excited at a frequency f_e approximately equal to f_s, the vortex pairing cascade contains sufficient energy to interact strongly with the column instability, provided that the two modes share a common frequency. The excitation frequency f_e for which optimum interaction occurs will be equal to the shear-layer instability frequency f_s only if the shear-layer properties are such that $f_s/8=f_j$, the frequency selected by the column independently. Otherwise, the optimum frequency will be at an intermediate value between f_s and $8f_j$. If the separation in frequencies is large, coupling will be weaker. When the shear-layer instability waves are disturbed by boundary-layer tripping, as in the case reported by Crow and Champagne,[1] the jet-column frequency reported was $St=0.3$. From Fig. 5, the nonexcited jet-column instability frequency was $f_j D/U=0.37$; with excitation the optimum interaction occured at $f_e D/8U=0.47$. The independent column instability frequency is inferred to be less

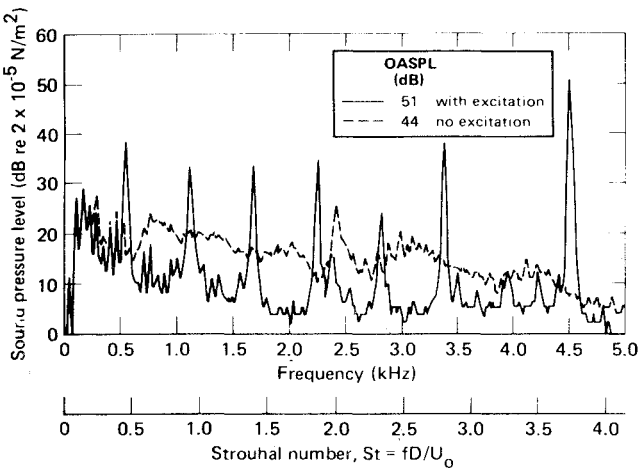

Fig. 8 Acoustic pressure spectrum at (50,40); $U_0 = 30.5$ m/s; $f_e = 4525$ Hz.

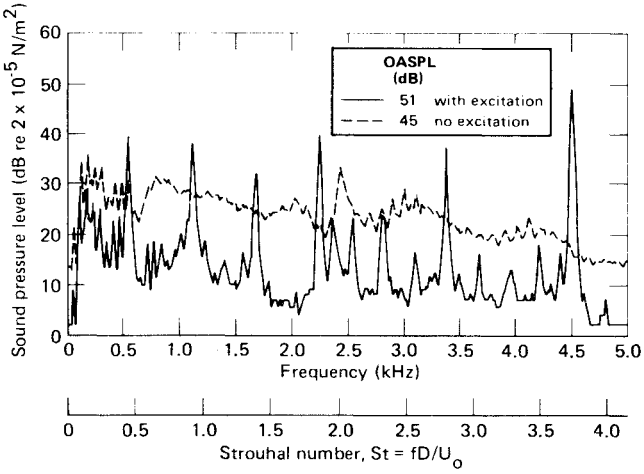

Fig. 9 Acoustic pressure spectrum at (50,30); $U_0 = 30.5$ m/s; $f_e = 4525$ Hz.

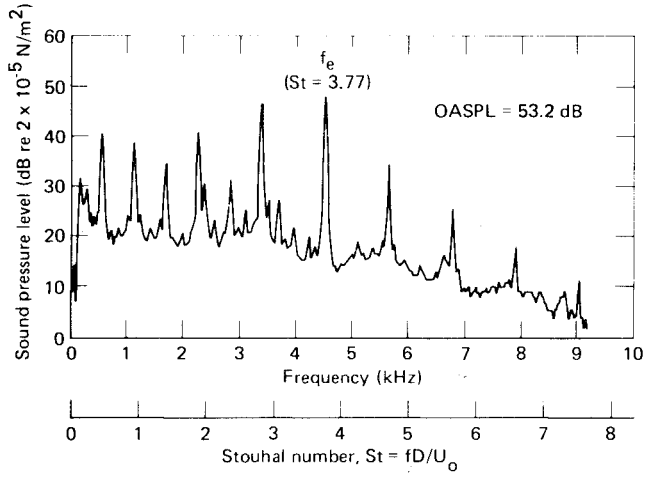

Fig. 10 Acoustic pressure spectrum at (10,30); $U_0 = 30.5$ m/s; $f_e = 4525$ Hz.

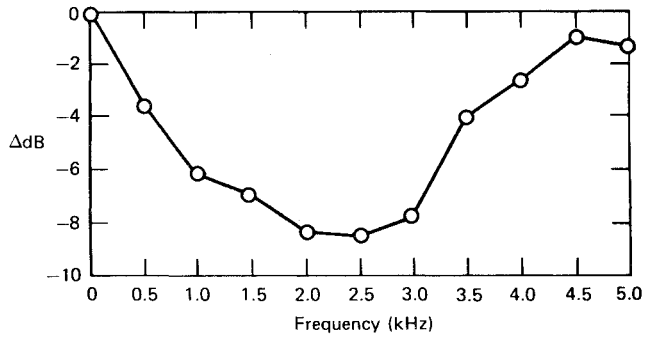

Fig. 11 Reduction of broadband component of sound pressure spectrum by excitation; $R/D = 30$, $U_0 = 30.5$ m/s; $f_e = 4525$ Hz; averaged over microphone positions $x/D = 0,10,20,30,40,50$.

than $St = 0.37$. An exact match would be expected by employing a jet with a thicker initial boundary layer for which $f_s/8 = f_j$.

The series of spectra shown in Figs. 6-9 illustrates the characteristics of the far acoustic field for $Re = 52{,}000$. The far-field spectrum is essentially discrete for the excited case. The spectrum peaks in the far field correspond exactly to those at the reference microphone position. Thus, the appearance of subharmonics of the excitation frequency in the acoustic field must be associated with the vortex pairing events in the shear layer. Since each of the three pairing events is constrained to a fixed streamwise location by the excitation process, the noise-source locations for the spectrum peaks at frequencies $f_e/2$,$f_e/4$, and $f_e/8$ are inferred to be those regions of the jet for which these frequencies were observed in the flowfield. The far-field acoustic spectrum, however, is not dominated by the peak at $f_e/8$ as was the near field. The energy levels at $f_e/2$,$f_e/4$, and $f_e/8$ are such that no single frequency dominates the entire far field. The peak at $f_e/2$ radiates strongly in the 90-deg direction, as indicated in Fig. 6. The effect of excitation on the sound pressure level in the far field is twofold. The overall sound pressure level (OASPL) increases by 4 to 8 dB. At the same time, the broadband component of the spectrum is suppressed, in some cases by more than 10 dB at selected frequency bands as shown in Fig. 9. The overall increase, therefore, is attributable to the discrete portion of the spectrum produced by the vortex ring cascade in the shear layer and the enhanced jet-column contribution at the frequency $f_e/8$. For $Re = 52{,}000$ the increase in OASPL and the corresponding decrease in the broadband noise were consistently exhibited throughout the far field with positional variations as indicated in Figs. 6-9. All far-field spectra for the nonexcited case, of which those shown in Figs. 6-9 are a sample, exhibit a consistent peak, approximately 8 db above the local broadband level, at a frequency $St = 2.00$. The first pairing event in the nonexcited case is the only part of the coherent motion that contains an energy level comparable to that in the excited jet, and, therefore, is the only one expected to radiate a discrete spectrum peak to the far field. The value of the first pairing frequency, $St = 2.00$, is higher than $f_e/2$, which is in agreement with the preceding argument concerning the inequality of $f_s/8$ and f_j.

The peaks attributable to interactions between the vortex passage frequencies appear in the spectrum above the frequency f_e as well and are shown in Fig. 10. For $f > f_e$, however, the sequence of peaks appears in steps of $f_e/4$.

In Fig. 11 the reduction of the broadband sound pressure level by excitation is plotted as a function of frequency for $R/D = 40$, averaging over all six microphone positions. The suppression of broadband noise was greatest in the mid-frequency range spanning the passage rates of the intermediate scales. Since the organization in the far-field spectrum is a direct reflection of the imposed organization in the flowfield, the midrange of the spectrum can be associated with the flowfield characteristics from $0.5 \leq x/D \leq 1.5$ where the corresponding frequencies are observed. Whereas in the nonexcited jet the contribution from this region to the acoustic spectrum was largely random, excitation organized the flowfield and thereby suppressed the random components in the spectrum.

Table 1 Cross-correlation coefficients

Microphone position	Center frequency	Cross-correlation coefficients Excit. off	Excit. on
(30,30)	Wide band	0.07	0.17
(30,30)	550 Hz	0.28	0.50
(30,30)	1100 Hz	0.10	0.72
(0,30)	Wide band	0.12	0.21
(0,30)	550 Hz	0.38	0.71
(0,30)	1100 Hz	0.18	0.45

Figure 12 shows the broadband cross-correlation coefficients $R_{12}=(p_1(t)p_2(t-\tau))/(p_1'p_2')$ formed from the reference microphone signal and those of microphones located at positions $(x/D, R/D)=(30,30)$ and (0,30) for the excited case. The curves are periodic with a period corresponding to that of $f_e/8$, indicating that for wideband cross-correlation, the lowest frequency in the spectrum is dominant. The maximum wideband correlation coefficient was 0.21. Furthermore, narrowband cross-correlation coefficients were measured for the filter center frequencies 550 Hz and 1100 Hz, corresponding to $f_e/8$ and $f_e/4$. The

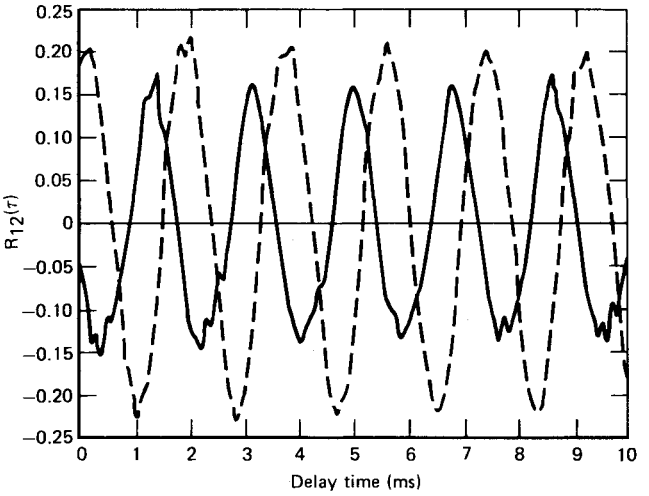

Fig. 12 Wide-band cross-correlation coefficient, $R_{12}(\tau)$; microphones correlated are at positions:—(0,1) and (30,30); --- (0,1) and (0,30).

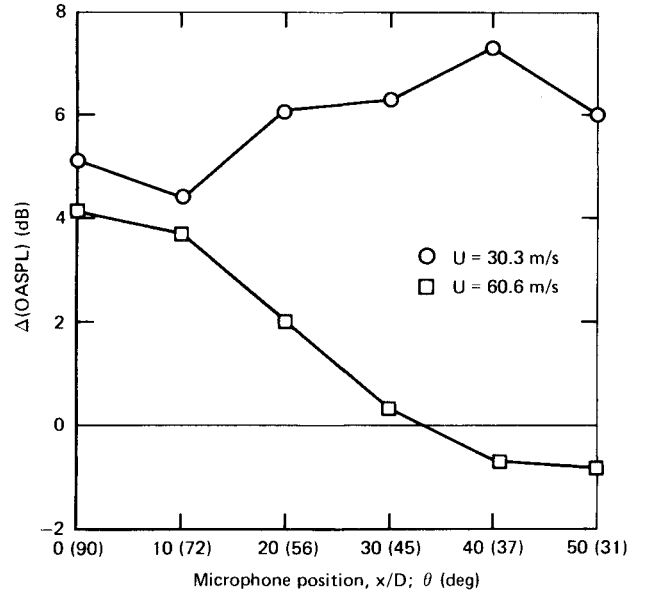

Fig. 13 Differences in OASPL of excited and nonexcited jets; $R/D=30$.

values of R_{12} are given in Table 1 for the excited and nonexcited cases. Correlation coefficients as high as 0.72 were recorded.

The increase in OASPL for the low-speed case is shown in Fig. 13 for $R/D=30$ as a function of the microphone position, or, alternatively as a function of angle θ with respect to jet axis. The maximum is at $\theta\cong 35$ deg indicating that the overall contribution to the acoustic field by the large-scale shear-layer structures is largest in this direction.

Figure 13 also shows directionality properties for the higher speed flow, i.e., $Re=104{,}000$. The increase in OASPL parallels that for the lower speed case for acoustic radiation perpendicular to the flow but decreases with θ and becomes negative for $\theta\approx 45$ deg. This behavior contrasts with that for the lower speed case and would at first glance seem to be unwarranted because both flows are at low-subsonic regimes. To explain this anomaly, compare the two cases in the near and far pressure fields. The higher speed pressure spectrum at the position (1,1) is shown in Fig. 14; it differs in several aspects from that for the lower speed case. First, the excitation frequency that was matched to the experimentally observed instability frequency for the higher speed jet, was 13,240 Hz, or $St=5.50$. Since a triple pairing process in this case would yield a frequency $St=0.69$, we would expect a weak interaction between the shear layer and jet instability modes as confirmed by the information in Fig. 14. Instead of enhancing the low-frequency end of the spectrum as in the lower speed case, excitation suppressed it by some 2 dB; excitation had no effect on the width of the peak, and the

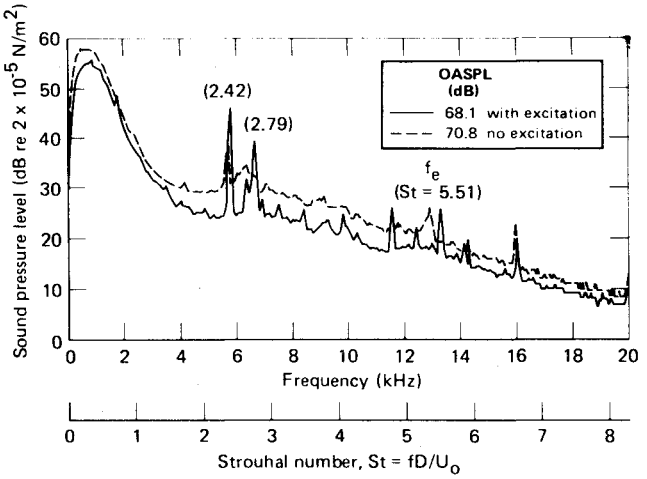

Fig. 14 Fluctuating pressure spectrum at (1,1); $U_0=60.6$ m/s; $f_e=13{,}240$ Hz.

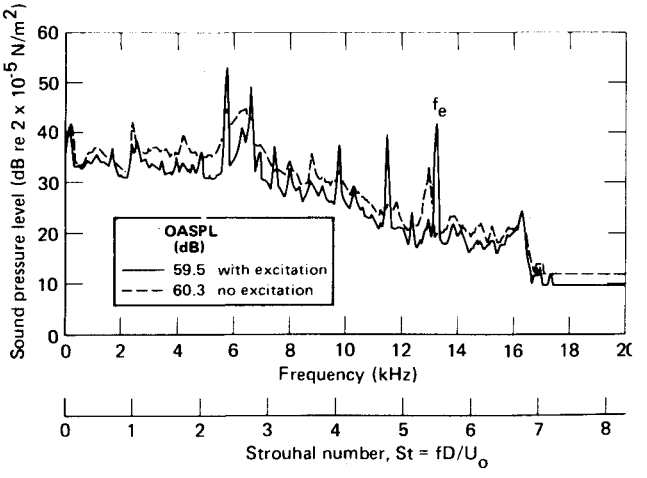

Fig. 15 Acoustic pressure spectrum at (50,30); $U_0=60.6$ m/s; $f_e=13{,}240$ Hz.

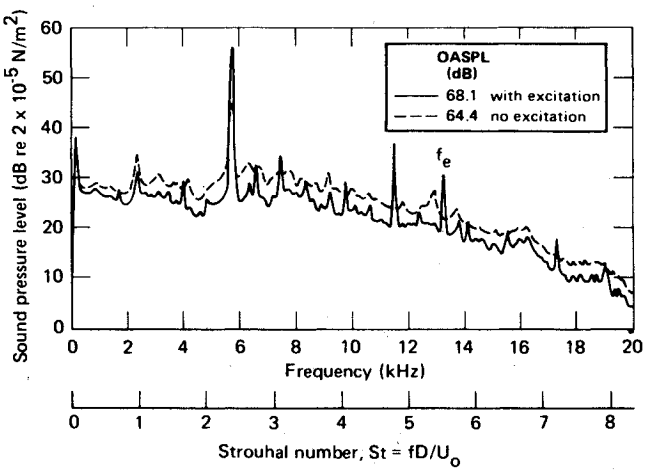

Fig. 16 Acoustic pressure spectrum at (10,30); $U_0 = 60.6$ m/s; $f_e = 13{,}240$ Hz.

frequency at which the maximum occurred remained unchanged. The low-frequency peak in this case was at $St = 0.30$, indicating that the jet-column mechanism was independent of the shear-layer development. Spectrum peaks appeared at $St = 2.79$ and 2.42 in response to excitation. The first value corresponds to one-half of the excitation frequency, but the second appeared at a frequency for which a smaller peak appeared also for the nonexcited case. The broadband pressure level decreased by a maximum of 5 dB in the mid-frequency range. The overall pressure level decreased by 2.7 dB.

The far-field spectra were qualitatively similar to those for the near field. In Fig. 15 at a microphone position corresponding to $\theta = 31$ deg, radiation at discrete frequencies is indicated for $St = 2.4$ and 2.8 which correspond to the peaks in the near-field spectrum. OASPL decreased by 0.8 dB upon excitation. For $\theta = 72$ deg (Fig. 16), a strong peak at $St = 2.4$ dominates the spectrum, and the OASPL increases with excitation by 3.7 dB.

The far-field spectra were qualitatively similar to those for the near field. In Fig. 15 at a microphone position corresponding to $\theta = 31$ deg radiation at discrete frequencies is indicated for $St = 2.4$ and 2.8 which correspond to the peaks in the near-field spectrum. OASPL decreased by 0.8 dB upon excitation. For $\theta = 72$ deg (Fig. 16), a strong peak at $St = 2.4$ dominates the spectrum, and the OASPL increases with excitation by 3.7 dB.

We conclude, therefore, that for the higher speed case, the excited shear layer suppressed broadband radiation in proportion to the degree that the large-scale structures in the shear layer were more organized than in the nonexcited case. The acoustic radiation efficiency of the organized structures in this case, however, was weak, and the overall effect on the far field was to lower the OASPL, except for θ near 90 deg.

Conclusions and Discussion

The shear layer was perturbed by an excitation signal at the shear-layer instability frequency whose amplitude was infinitesimal compared with the gross exit-plane fluid dynamic parameters. The phase coherence provided by the signal enabled the shear-layer structure to develop into a deterministic sequence of periodic vortex pairing events at fixed positions in the shear layer. The organization imposed on the flowfield reduced the jitter of the pairing events and increased the energy contained by the coherent motion. The resulting highly ordered vortex-pairing cascade generated acoustic waves which propagated to the far field. The frequencies observed in the far field corresponded exactly to the vortex-formation frequencies in the flowfield, and the broadband noise was reduced. Narrow-band cross-correlation coefficients as high as 0.72 were recorded. These results suggest that the jet flow supports two independent but interacting oscillation mechanisms, namely the shear layer and the column modes, and that for selected frequency ranges, the noise-generation characteristics of the jet reflect the interaction of both mechanisms. The disparity in the column instability frequencies measured in various facilities may result from variations in the degree of interaction between these two mechanisms.

The observed decrease in the broadband noise is opposite to the result observed by Bechert and Pfizenmaier[15] and by Moore.[16] The difference in the results may be explained as follows. The broadband decrease was largest for the mid-frequencies corresponding to the rates of formation of the intermediate scales in the shear layer. In the present experiment, the source locations for these frequencies were rigidly fixed by the excitation scheme employed. In the experiments employing excitation in the form of sinusoidal planar surging at $St = 0.5$, for example, only the jet-column mechanism is enhanced directly. The interaction between the excited column oscillations and the shear layer appears to introduce a net increase in the jitter of the pairing locations in the shear layer, and rather than producing discrete tones, the enhanced shear-layer motion increases the broadband noise.

These experimental results show that under controlled conditions vortex pairing can constitute a major generating mechanism for jet noise as well as influence noise-emission characteristics at low frequencies through the interaction of the shear layer and jet column instability modes of oscillation.

Acknowledgments

The contributions to this study by D.H. Hickey and P.T. Soderman of NASA Ames Research Center and by D. Stouder, J. Morgan and D. Johnson of the Douglas Aircraft Company Acoustics and Vibration Data Center are gratefully acknowledged. This research was conducted under the McDonnell Douglas Independent Research and Development Program in cooperation with NASA Ames Research Center.

References

[1] Crow, S.C. and Champagne, F.H., "Orderly Structure in Jet Turbulence," *Journal of Fluid Mechanics,* Vol. 48, Aug. 1971, pp. 547-591.

[2] Winant, C.D. and Browand, F.K., "Vortex Pairing: The Mechanism of Turbulent Mixing-Layer Growth at Moderate Reynolds Number," *Journal of Fluid Mechanics,* Vol. 63, April 1974, pp. 237-255.

[3] Brown, G.L. and Roshko, A., "On Density Effects and Large Structures in Turbulent Mixing Layers," *Journal of Fluid Mechanics,* Vol. 64, July 1974, pp. 775-816.

[4] Browand, F.K. and Weidman, P.D., "Large Scales in the Developing Mixing Layer," *Journal of Fluid Mechanics,* Vol. 76, July 1976, pp. 127-144.

[5] Browand, F.K., Chu, W.T., and Laufer, J., "Exploratory Experiments on the Entrance Effects in Subsonic Jet Flows," Rept. USCAE 130, Univ. of Southern Calif., 1975.

[6] Michalke, A. and Fuchs, H.V., "On Turbulence and Noise of an Axisymmetric Shear Flow," *Journal of Fluid Mechanics,* Vol. 70, July 1975, pp. 179-205.

[7] Fuchs, H.V. and Michel, U., "Experimental Evidence of Turbulent Source Coherence Affecting Jet Noise," *AIAA Journal,* Vol. 16, Sept. 1978, pp. 871-872.

[8] Sarohia, V. and Massier, P.F., "Experimental Results of Large-Scale Structures in Jet Flows and Their Relation to Jet Noise Production," AIAA Paper 77-1350, Oct. 1977; also *AIAA Journal,* Vol. 16, Aug. 1978, pp. 831-835.

[9] McLaughlin, D.K., Morrison, G.L., and Troutt, T.R., "Reynolds Number Dependence in Supersonic Jet Noise," *AIAA Journal,* Vol. 15, Aug. 1977, pp. 526-532.

[10] Lau, J.C., Fisher, M.J., and Fuchs, H.V., "The Intrinsic Structure of Turbulent Jets," *Journal of Sound and Vibration,* Vol. 22, June 1972, pp. 379-406.

[11] Maestrello, L., "Statistical Properties of the Sound and Source Fields of an Axisymmetric Jet," AIAA Paper 77-1267, 1977.
[12] Petersen, R.A., Kaplan, R.E. and Laufer, J., "Ordered Structures and Jet Noise," NASA CR-134733, 1974.
[13] Zaman, K.B.M.Q. and Hussain, A.K.M.F., "Vortex Pairing and Organized Structures in Axisymmetric Jets under Controlled Excitation," Proceedings of Symposium on Turbulent Shear Flow, Penn. State Univ. April 1977, 11:23-11:31.
[14] Chan, Y.Y., "Spatial Waves of Higher Modes in an Axisymmetric Turbulent Jet," *The Physics of Fluids,* Vol. 19, Dec. 1976, pp. 2042-2043.
[15] Bechert, D. and Pfizenmaier, E., "On the Amplification of Broadband Jet Noise by a Pure Tone Excitation," *Journal of Sound Vibration,* Vol. 43, Dec. 1975, pp. 581-587.
[16] Moore, C.J., "The Role of Shear-layer Instability Waves in Jet Exhaust Noise," *Journal of Fluid Mechanics,* Vol. 80, April 1977, pp. 321-367.
[17] Michalke, A., "The Instability of a Compressible Circular Jet with Finite Boundary Layer Thickness," in German, Zeitschrift fur Flugwissenschaften, Vol. 19, Aug./Sept. 1971, pp. 319-327.
[18] Laufer, J. and Monkewitz, P.A., "The Influence of the Dominant Large-Scale Structures on the Initial Instability of a Low-Speed Circular Jet," *Bulletin of the American Physical Society,* Vol. 23, Oct. 1978, p. 1004.
[19] Kibens, V., "Noise Generated by Large-Scale Structures in an Axisymmetric Jet," *Bulletin of the American Physical Society,* Vol. 23, Oct. 1978, p. 1015.